

# EMPLOYING TWIN CRABBING CAVITIES TO ADDRESS VARIABLE TRANSVERSE COUPLING OF BEAMS IN THE MEIC\*

A. Castilla<sup>1,2,3†</sup>, V. S. Morozov<sup>2</sup>, T. Satogata<sup>1,2</sup>, J. R. Delayen<sup>1,2</sup>.

<sup>1</sup>Center for Accelerator Science, Old Dominion University, Norfolk, VA 23529, USA.

<sup>2</sup>Thomas Jefferson National Accelerator Facility, Newport News, VA 23606, USA.

<sup>3</sup>Universidad de Guanajuato (DCI-UG), Departamento de Fisica, Leon, Gto. 37150, Mex.

## Abstract

The design strategy of the Medium Energy Electron-Ion Collider (MEIC) at Jefferson Lab considers both the matching of the beam spot sizes at collision and a 50 mrad crossing angle along with crab crossing scheme for both electron and ion beams over the energy range ( $\sqrt{s} = 20 - 70$  GeV) to achieve high luminosities at the interaction points (IPs). However, the desired locations for placing the crabbing cavities may include regions where the transverse degrees of freedom of the beams are coupled with variable coupling strength that depends on the collider rings' magnetic elements (solenoids and skew quadrupoles). In this work we explore the feasibility of employing *twin* rf dipoles that produce a variable direction crabbing kick to account for a range of transverse coupling of both beams.

## INTRODUCTION

Due to spacial and technical restrictions on the MEIC lattice, high  $\beta$  regions with transverse coupled beams are being considered as locations for the crabbing cavity correctors [1]. In this academic exercise we have used simple analytical methods to evaluate the effects of the solenoid field in the interaction region (IR). By backtracking the bunches to the crabbing cavity locations, we have determined the proper kick angle needed to produce the desired horizontal crossing orientation of the colliding bunches at the IP. We have considered basic setups to account for the variable coupling in the crossing correction scheme to restore luminosity degradation in the machine. The setup we focus on, involves the use of double (*twin*) crabbing cavities that can provide an effective variable angle kick within the needed range to compensate for the beam energy dependent transverse coupling.

## Definitions

For this first study we considered only the linear effects of the solenoids [2], crabbing cavities and of the quadrupoles composing the final focusing blocks (FFB) [3]. We use the following notation in the transfer matrix [4]: with  $F$  is the focal length,  $D$  is the drift length,  $C \equiv \cos(KL)$ ,  $S \equiv \sin(KL)$ ,  $K \equiv \frac{qB_{Sol}}{2P}$  where  $q$  is the

particle charge,  $B_{Sol}$  is the solenoid magnetic induction,  $P$  is the particle's momentum, and  $L$  is the solenoid length.

## TRANSVERSE BASIS ROTATION

The transfer matrix from the crabbing cavity location towards the interaction point (IP) with the crabbing kicker off, can be written as:

$$\mathbb{M}_{T2} = \mathbb{M}_{SOL}\mathbb{M}_L\mathbb{M}_{FFB}; \quad (1)$$

where  $\mathbb{M}_{SOL}$ ,  $\mathbb{M}_L$ , and  $\mathbb{M}_{FFB}$  represent the thin-like lens transfer matrices for solenoid, drift, and final focusing block respectively. With the transverse basis at the IP given by:  $\hat{x}^T = (1, 0, 0, 0, 0, 0)$ , and  $\hat{y}^T = (0, 0, 1, 0, 0, 0)$ .

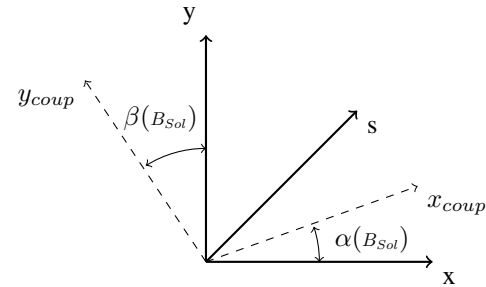


Figure 1: Transverse coordinate basis at the IP (solid) and coupled transverse coordinate basis at the crabbing cavity position (dashed), where  $B_{Sol}$  is the solenoid field strength.

To back propagate the IP's transverse coordinate basis towards the crabbing cavity position, we established a new set of transverse coordinates at the location of the crabbing cavity ( $\hat{x}_{coup}$ ,  $\hat{y}_{coup}$ ) as a linear transformation of the original transverse basis at the IP (See Fig. 1):

$$\begin{Bmatrix} \hat{x}_{coup} \\ \hat{y}_{coup} \end{Bmatrix} = \mathbb{M}_{T2}^{-1} \begin{Bmatrix} \hat{x} \\ \hat{y} \end{Bmatrix}; \quad (2)$$

where with  $T \equiv \tan(KL)$ :

$$\mathbb{M}_{T2}^{-1} = \begin{pmatrix} C(C-DKS) & -\frac{C^2(DK+T)}{K} & S(DKS-C) & \frac{S(DKC+S)}{K} & 0 & 0 \\ \frac{C(C+(F-D)KS)}{F} & -\frac{C^2((D-F)K+T)}{FK} & -\frac{S(C+(F-D)KS)}{F} & \frac{S((D-F)KC+S)}{FK} & 0 & 0 \\ S(C-DKS) & -\frac{S(DK+C+S)}{K} & C(C-DKS) & -\frac{C^2(DK+T)}{K} & 0 & 0 \\ \frac{S(C+(F-D)KS)}{F} & -\frac{S((D-F)KC+S)}{FK} & \frac{C(C+(F-D)KS)}{F} & -\frac{C^2((D-F)K+T)}{FK} & 0 & 0 \\ 0 & 0 & 0 & 0 & 1 & 0 \\ 0 & 0 & 0 & 0 & 0 & 1 \end{pmatrix}.$$

\* Authored by Jefferson Science Associates, LLC under U.S. DOE Contract No. DE-AC05-06OR23177.

† acastill@jlab.org

Plugging this into Eq. 2, we get:

$$\begin{aligned}\hat{x}_{coup}^T &= (C(C - DKS), x'_x, S(C - DKS), y'_x, 0, 0), \\ \hat{y}_{coup}^T &= (-S(C - DKS), x'_y, C(C - DKS), y'_y, 0, 0).\end{aligned}$$

Once again using this result and the diagram of Fig. 1, we could determine the horizontal and vertical angles as:

$$\tan(\alpha) = \frac{S(C - DKS)}{C(C - DKS)} = \tan(\beta) = T. \quad (3)$$

## CALCULATIONS

### Mixing Angle

We analyzed the behavior of the mixing angle  $KL$ , both for electrons ( $P_e = 5$  GeV,  $D_e = 4$  m,  $F_e = 7$  m, and  $L_e = 3$  m) and protons ( $P_p = 60$  GeV,  $D_p = 5$  m,  $F_p = 7$  m, and  $L_p = 2$  m), as a function of  $B_{Sol}$  in Fig. 2 taking into account the upstream and downstream asymmetry of the IP [3].

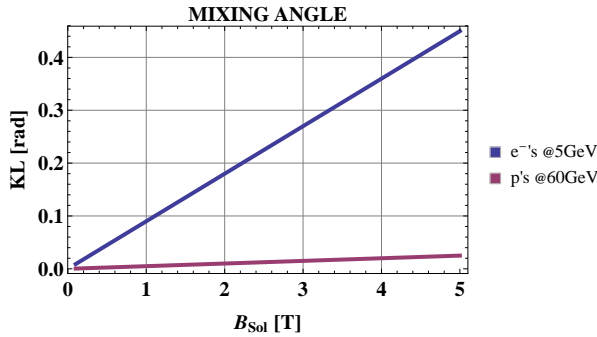


Figure 2: Magnitude of  $KL$  in radians for electrons (blue), and protons (purple) at the position of the crabber.

Examples of the coupled transverse distributions both for electrons and protons for several values of  $B_{Sol}$  are presented in Figs. 3 and 4 respectively:

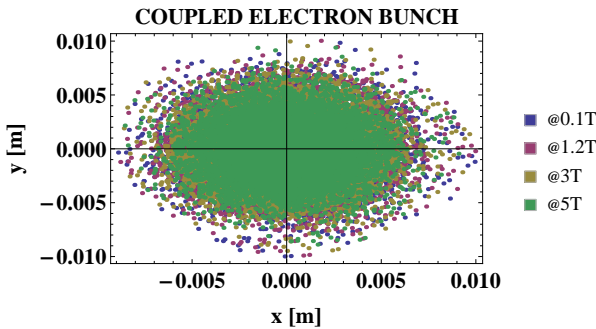


Figure 3: Electron distributions at the crabber location for different  $B_{Sol}$  @5GeV,  $D_e + L_e = F = 7$  m.

### Rotated Crabbing Cavity

A crabbing cavity rotated by  $KL$  about the  $z$  axis (i.e.  $\mathbb{M}_{C,\Sigma} = \mathbb{R}(-KL)\mathbb{M}_C\mathbb{R}(KL)$  [4]) will give a kick in the

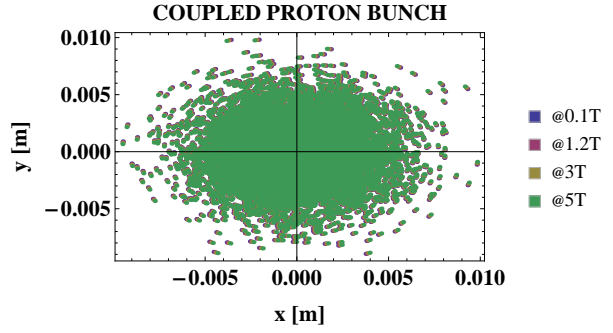


Figure 4: Proton distributions at the crabber location for different  $B_{Sol}$  @60GeV,  $D_p + L_p = F = 7$  m.

“correct” direction at the crabbing cavity location to produce the desired crabbed distributions at the IP. The transfer matrix for such a rotated crabber can be seen in Eq. 4.

$$\mathbb{M}_{C,\Sigma} = \begin{pmatrix} 1 & 0 & 0 & 0 & 0 & 0 \\ 0 & 1 & 0 & 0 & \frac{C \tan(\phi_C)}{F} & 0 \\ 0 & 0 & 1 & 0 & 0 & 0 \\ 0 & 0 & 0 & 1 & \frac{S \tan(\phi_C)}{F} & 0 \\ 0 & 0 & 0 & 0 & 1 & 0 \\ \frac{C \tan(\phi_C)}{F} & 0 & \frac{S \tan(\phi_C)}{F} & 0 & 0 & 1 \end{pmatrix}. \quad (4)$$

The crabbing angle in the MEIC is  $\phi_C = 25$  mrad per bunch. We can use this to find the total transfer matrix as  $\mathbb{M}_{C\Sigma T} = \mathbb{M}_{T2}\mathbb{M}_{C,\Sigma}$ .

We plot the distributions propagated through  $\mathbb{M}_{C\Sigma T}$  to the IP for different values of  $B_{Sol}$  in Figs. 5 (a) and (b) for electrons and protons, respectively.

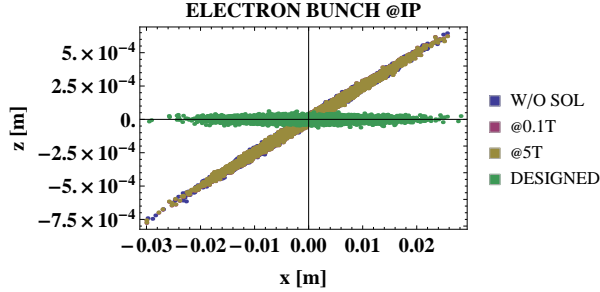
A plot of the crabbing angle as a function of  $B_{Sol}$ , in Fig. 6 both for the electron ( $P_e = 5$  GeV,  $D_e = 4$  m, and  $L_e = 3$  m), and proton ( $P_p = 60$  GeV,  $D_p = 5$  m, and  $L_p = 2$  m) bunches, with  $F = 7$  m, shows that the maximum error in the crabbing angle due to additional solenoid focusing is  $\sim 7\%$  for electrons and  $< 0.1\%$  for protons in the studied  $B_{Sol}$  range. This extra focusing will be compensated by the FFB’s quadrupoles.

## TWINING THE CRABBERS

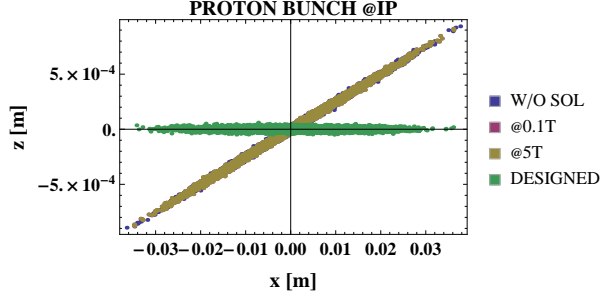
As a final step, we studied an array of 2 *twin* cavities  $\vec{C}_{x1}$  and  $\vec{C}_{x2}$ , whose superposition simulates a variable angle ( $\theta_{coup}$ ) crabbing kick  $\vec{C}_{\Sigma} = \vec{C}_{x1} + \vec{C}_{x2}$ , that will account for the transverse coupling of the beams. Then, using Fig. 7 and the cosine theorem, we can write down the effective kick as:

$$\begin{aligned}\vec{C}_{\Sigma} &= [C_{x1} \cos(\theta_{coup} - \alpha_{x1}) + C_{x2} \cos(\alpha_{x2} - \theta_{coup})] \\ &\times [\cos(\theta_{coup})\hat{x} + \sin(\theta_{coup})\hat{y}],\end{aligned} \quad (5)$$

Fig. 8 shows how when optimizing to balance the voltage needed from the *twins*  $C_{x1}$  and  $C_{x2}$  (left) to obtain the desired kick, the *twins* are found to be parallel, thus we lose angular coverage to a single coupling angle  $\theta_{coup}$ . And



(a) Electron distributions.



(b) Proton distributions.

Figure 5: Electron (a) and proton (b) distributions at the IP for different  $B_{Sol}$ , using a crabber rotated by an angle of  $KL$ , compared to the case of the solenoid off (blue), and both the crabbing cavity and the solenoid off (green).

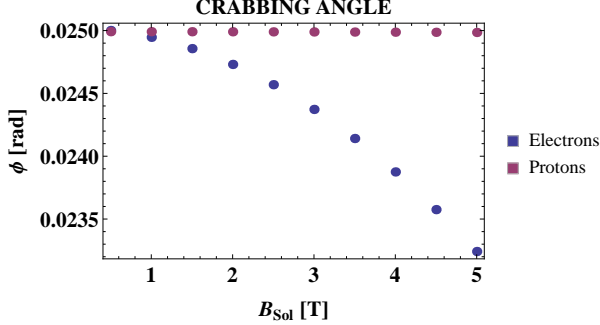


Figure 6: Total crabbing angle at the IP ( $\phi$ ) for electrons (blue) and protons (purple) as a function of the  $B_{Sol}$ .

when optimizing for a maximum angular coverage (right), we lose balance of the voltage contribution for the cavities. This trade off needs to be considered to find the optimal angle  $\theta_{twin}$ , that balances the *twins'* voltage contributions for the needed angular range ( $\theta_{coup} = KL$ ) in the MEIC.

## CONCLUSIONS

We proved analytically that an orthonormal transverse basis at the IP back propagated towards the crabbing cavity location considering a solenoid will still be an orthonormal, but rotated by an angle that depends on the solenoid strength as  $\theta_{coup}(B_{Sol}) = KL$ . Thus, for the MEIC in the case of electrons at 5 GeV, this angle changes from 0 to

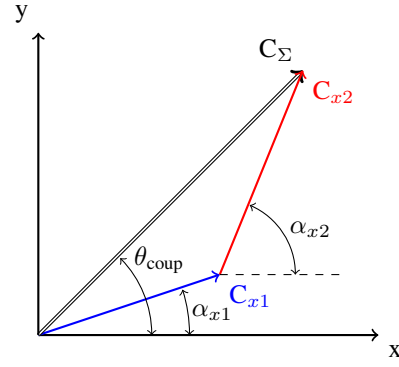


Figure 7: *Twin* crabbing kicks  $\vec{C}_{x1}$  (blue), and  $\vec{C}_{x2}$  (red) with  $\alpha_{x1}$  and  $\alpha_{x2}$  respectively, and the total kick  $\vec{C}_{\Sigma} = \vec{C}_{x1} + \vec{C}_{x2}$  (double lined), with a variable angle  $\theta_{coup}$ .

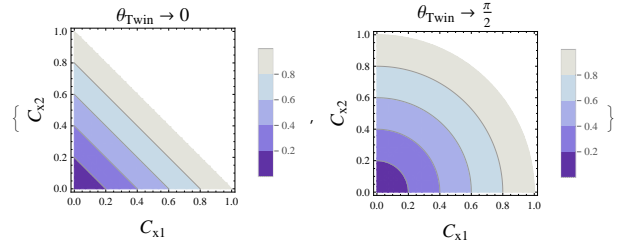


Figure 8:  $|\hat{C}_{\Sigma}|$  as a function of both *twins'* normalized amplitudes  $C_{x1}$  and  $C_{x2}$ , for the two extreme values of their relative angle  $\theta_{twin} \equiv \alpha_{x2} - \alpha_{x1} = 0$ , and  $\theta_{twin} = \frac{\pi}{2}$ .

$\sim \frac{\pi}{8}$  for a solenoid magnetic induction  $B_{Sol} \leq 5$  T. Also it is important to remark that all the contributions due to the angles and energy spreads have been neglected from the calculations for simplicity, since in this paper we did not propagate 6D bunch distributions but merely the 2D transverse coordinate system as a first approximation. We conclude that for the MEIC, an scheme of *twin* crabbing cavities that provides the proper kick for several angles in the necessary range for the various solenoid strengths is feasible, and the extra solenoid focusing has to be compensated by the FFB to avoid a maximum error on the crabbing angle of  $\sim 7\%$  for electrons, and  $< 0.1\%$ . Further studies will require consideration of the higher order contributions of the magnetic elements and particle tracking analysis.

## REFERENCES

- [1] R. B. Palmer, “Energy Scaling, Crab Crossing and The Pair Problem”, SLAC-PUB 4707. (1988).
- [2] F. Ciocci et al., “Generalized Twiss Coefficient Including Transverse Coupling and E-Beam Growth”, in Proceedings of EPAC 2006, Edinburgh, Scotland, p. 1966 (2006).
- [3] F. Lin et al., “Interaction Region Design and Detector Integration at JLab’s MEIC”, in Proceedings of PAC2013, Pasadena, California, p. 508 (2013).
- [4] A.W. Chao and M. Tigner, “Handbook of Accelerator Physics and Engineering” 3rd print, World Scientific Publishing Co. (2006).